Supporting Information

For

Modulation of the Calcium Oxalate Dihydrate to Calcium Oxalate Monohydrate Phase Transition by Citrate and Zinc Ions

Jing Zhang,[†] Wenjun Zhang,[†] Christine V. Putnis,[‡,§] and Lijun Wang[*,†]

[†]College of Resources and Environment, Huazhong Agricultural University, Wuhan 430070, China

[‡]Institut für Mineralogie, University of Münster, 48149 Münster, Germany

[§]School of Molecular and Life Science, Curtin University, 6845 Perth, Australia

SI TABLES (S1-S3)

SI FIGURES (S1-S6)

Table S1. Experimental conditions of the preparation of COD crystals with different concentrations of CA and Zn^{2+}.

Sample name	Additive	Solution A	pH of solution A	Solution B	pH of solution B
COD	-	80 mM $CaCl_2$	7	80 mM $K_2C_2O_4$	7
COD-CA2	citrate	80 mM $CaCl_2$	7	80 mM $K_2C_2O_4$ +4 mM $Na_3C_6H_5O_7$	7
COD-CA4	citrate	80 mM $CaCl_2$	7	80 mM $K_2C_2O_4$ +8 mM $Na_3C_6H_5O_7$	7
COD-CA8	citrate	80 mM $CaCl_2$	7	80 Mm $K_2C_2O_4$ +16 mM $Na_3C_6H_5O_7$	7
COD-Zn2	Zn^{2+}	80 mM $CaCl_2$+4 mM $ZnCl_2$	7	80 mM $K_2C_2O_4$	7
COD-Zn4	Zn^{2+}	80 mM Ca Cl_2+8 mM $ZnCl_2$	7	80 mM $K_2C_2O_4$	7
COD-Zn8	Zn^{2+}	80 mM Ca Cl_2+16 mM $ZnCl_2$	7	80 mM $K_2C_2O_4$	7

Table S2. Solution conditions for the COD to COM phase transformation.

Final solution concentration (mmol L^{-1})					
KCl	$CaCl_2$	$K_2C_2O_4$	$Na_3C_6H_5O_7$	$ZnCl_2$	$\sigma_{COD/COM}$
145	1.5	0.15	-	-	0.49/1.2
143	1.5	0.15	1	-	0.22/0.8
142	1.5	0.15	-	1	0.49/1.2
146	1.2	0.12	-	-	0.22/0.8

24

25

Table S3. Binding energies (eV) of C 1s, O 1s, Ca 2p and Zn 2p core levels of COD, COD-CA8 and COD-Zn8.

system	C 1s	O 1s	Ca $2p_{1/2}$	Ca $2p_{3/2}$	Zn $2p_{1/2}$	Zn $2p_{3/2}$
COD	284.8	531.7	350.8	347.3	-	-
COD-CA8	284.8	532.0	351.2	347.6	-	-
COD-Zn8	284.8	532.2	351.3	347.8	1046.7	1023.2

26

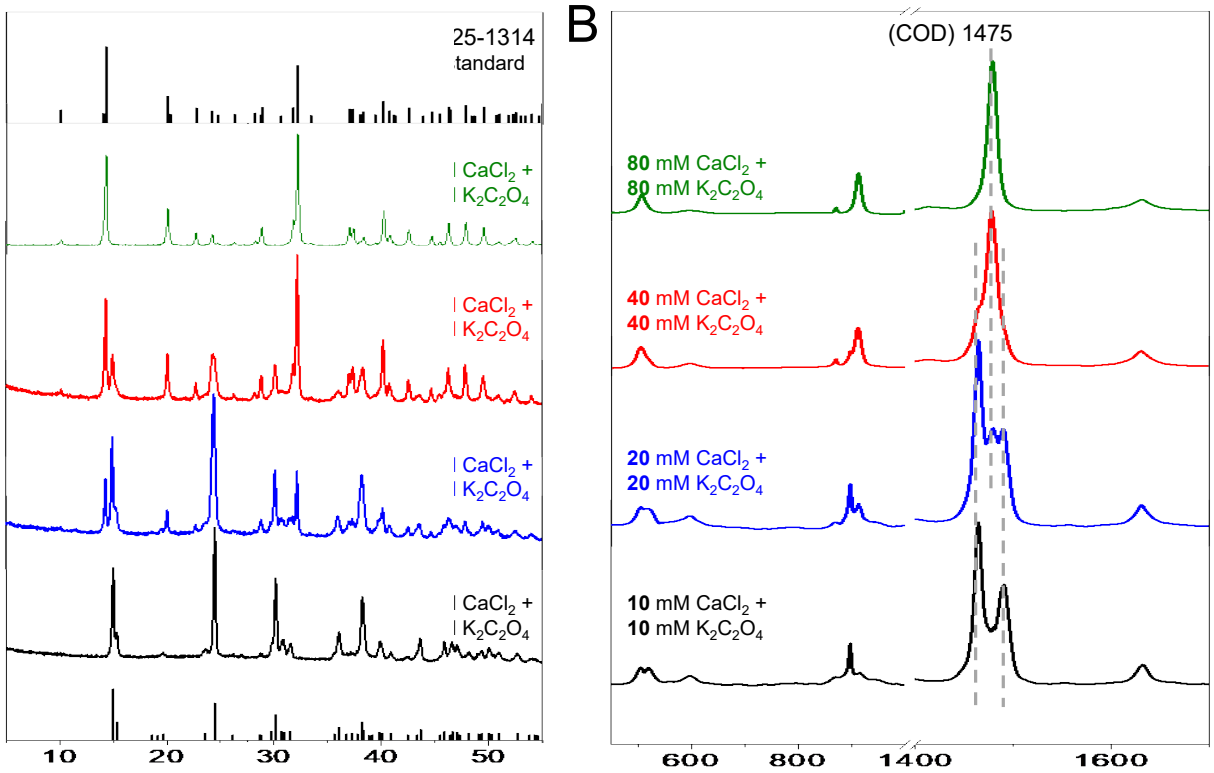

Figure S1. (A) XRD pattern and (B) Raman spectroscopic analysis of the precipitates prepared by quickly adding 10 mM (black), 20 mM (blue), 40 mM (red) and 80 mM (green) $K_2C_2O_4$ into the same concentration of $CaCl_2$ solutions.

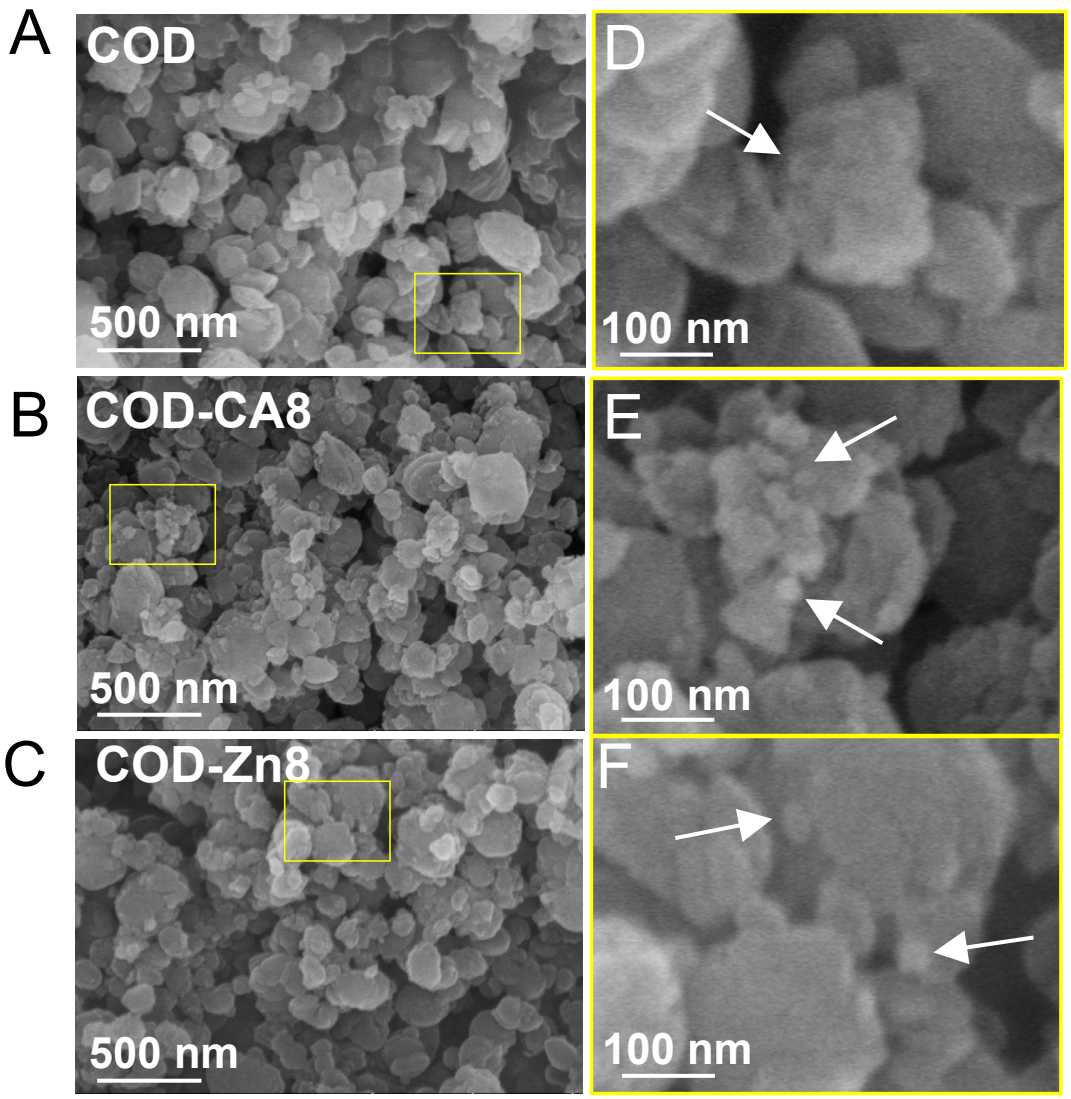

Figure S2. SEM images of freshly prepared crystals of (A) COD, (B) COD-CA8, and (C) COD-Zn8. (D-F) Magnified areas marked by yellow rectangles in (A), (B) and (C), respectively show that calcium oxalate precipitates are composed of smaller nanoparticles with sizes of 20-40 nm in diameter (highlighted by white arrows).

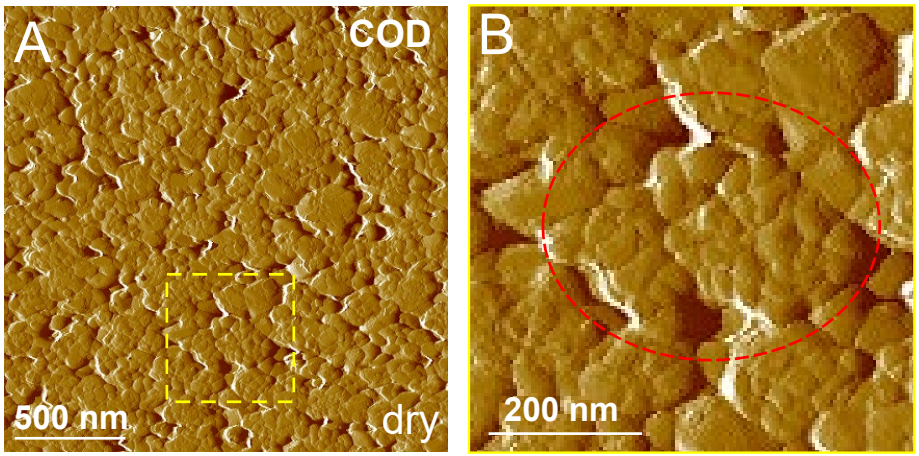

Figure S3. (A) AFM deflection image of freshly prepared COD crystals. (B) Magnified area marked by a yellow dotted rectangle in (A) shows that calcium oxalate precipitates (highlighted by red circle) are composed of smaller nanoparticles with sizes of 20-40 nm in diameter.

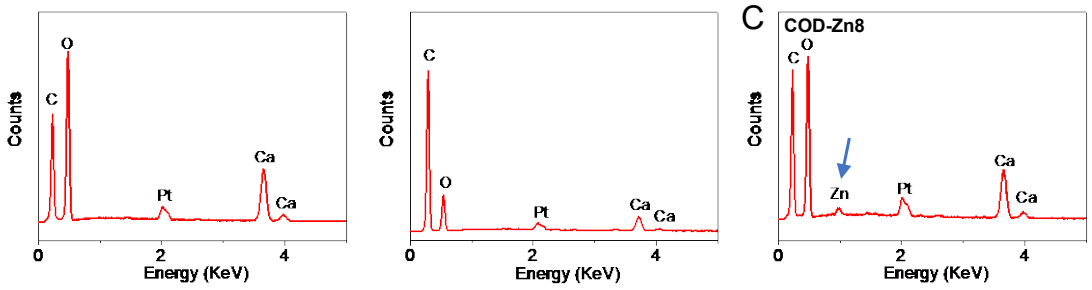

Figure S4. EDX spectrum of (A) COD, (B) COD-CA8 and (C) COD-Zn8 after 6 h of reaction in solutions containing 1.5 mM $CaCl_2$ and 0.15 mM $K_2C_2O_4$ at *IS* = 0.15 M and pH = 7.0 with no additives. All samples contain Ca, C and O. A blue arrow in (C) emphasizes the presence of Zn in COD-Zn8.The SEM images are shown in Figure 2C, 2F and 2I.

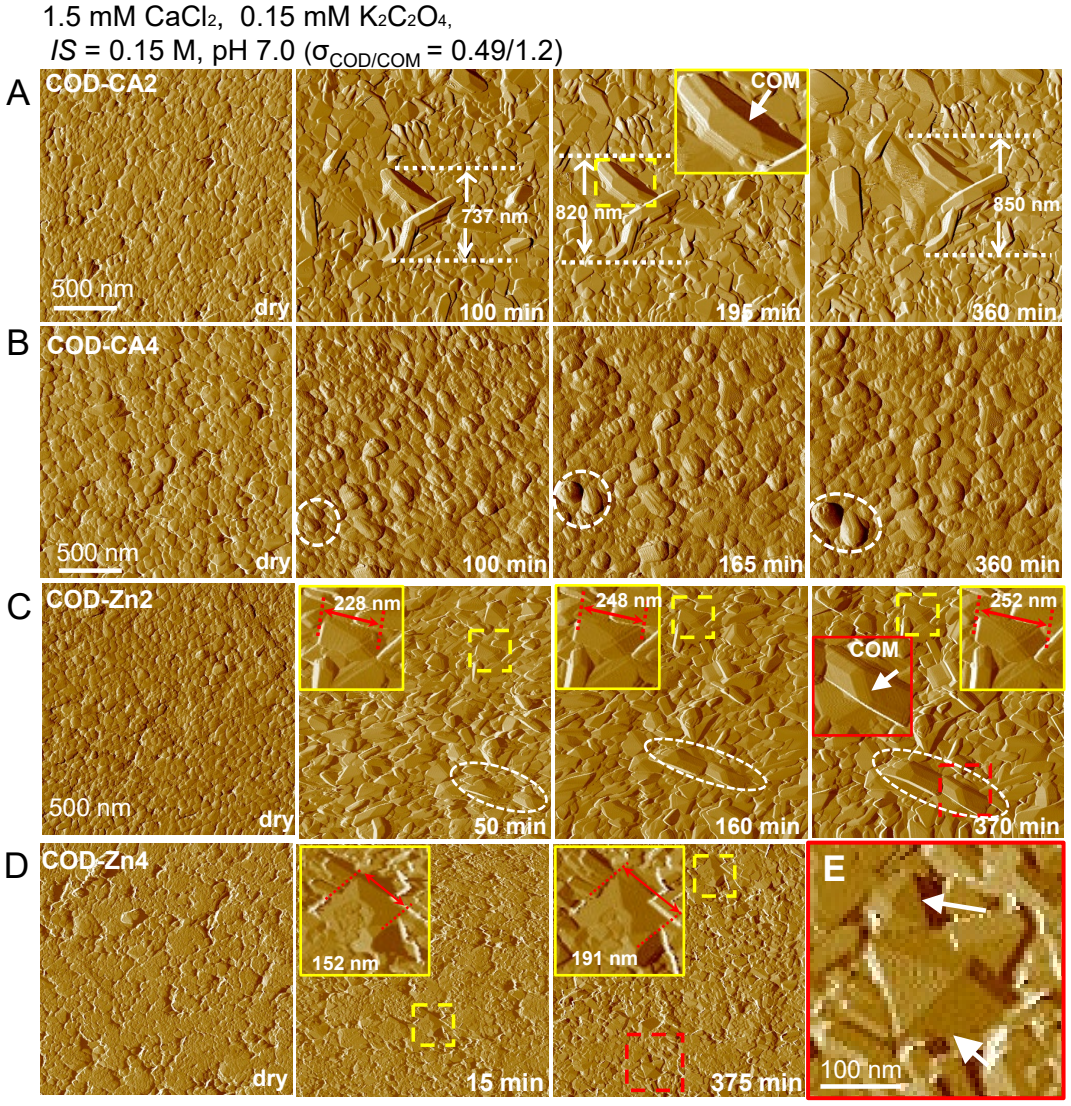

Figure S5. Time-resolved AFM deflection images show the *in situ* morphological evolution of (A) COD-CA2, (B) COD-CA4, (C) COD-Zn2 and (D) COD-Zn4 in a solution supersaturated with respect to CaOx (σ_{COD} = 0.49, 1.5 mM $CaCl_2$ and 0.15 mM $K_2C_2O_4$ at *IS* = 0.15 M and pH = 7.0). Inset in (A) shows a magnified area marked by a yellow dashed rectangle to indicate the presence of a typical COM crystal. White dashed lines and arrows in (A) demonstrate the growth of COM with elongated crystalline faces. White dashed circles in (B) emphasize that the crystals in this area gradually grow over time. Yellow insets in (C) demonstrate magnified areas marked by

the yellow dashed rectangles to show typical quadrangular pyramid-shaped COD crystals formed within 50 min of reaction and their slow growth. Red inset in (C) shows a magnified area marked by a red dashed rectangle to indicate the presence of a typical COM crystal. White dashed lines and arrows in (C) demonstrate the growth of COM with elongated crystalline faces. Insets in (D) demonstrate magnified areas marked by yellow rectangles to show typical quadrangular pyramid-shaped COD crystals rapidly formed within 15 min of reaction and their slow growth. (E) A magnification area marked by a red dotted rectangle in (D) clearly showing a quadrangular pyramid-shaped COD crystal (highlighted by white arrows).

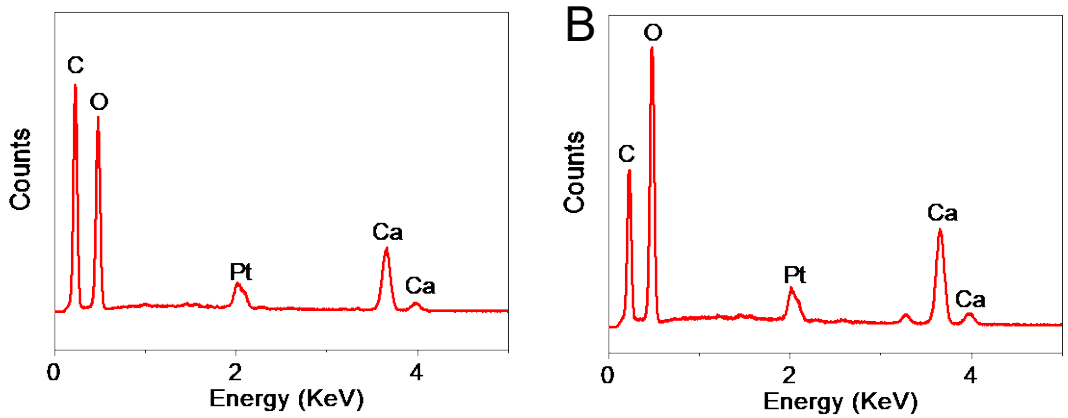

Figure S6. EDX spectrum of COD after 6 h of reaction in solutions containing 1.5 mM $CaCl_2$ and 0.15 mM $K_2C_2O_4$ at *IS* = 0.15 M and pH = 7.0 in the presence of (A) 1.0 mM sodium citrate ($Na_3C_6H_5O_7$) ($\sigma_{COD/COM}$ = 0.22/0.8) or (B) 1.0 mM $ZnCl_2$ ($\sigma_{COD/COM}$ = 0.49/1.2). All samples contain Ca, C and O. The SEM images are shown in Figure 3B and 3D.

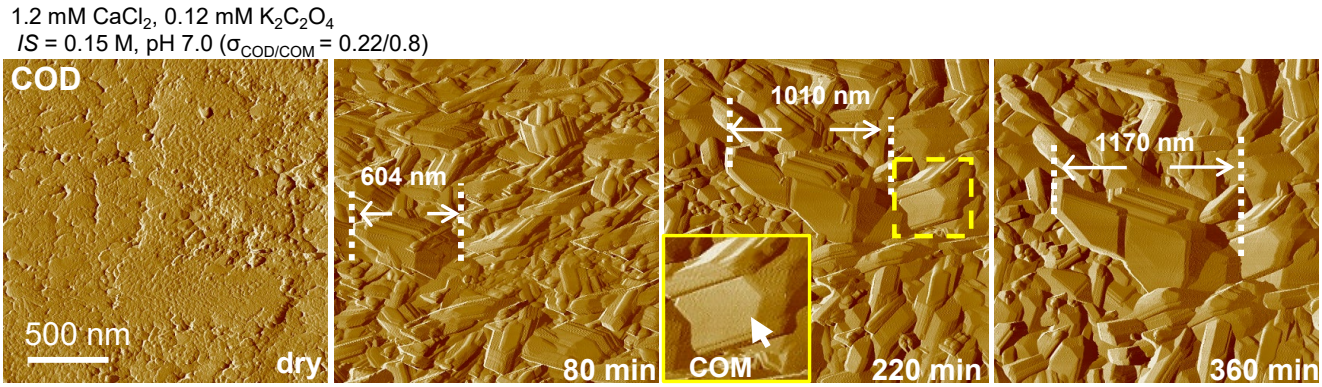

Figure S7. Time-resolved AFM deflection images show the *in situ* morphological evolution of COD in a solution supersaturated with respect to CaOx ($\sigma_{COD/COM}$ = 0.22/0.8, 1.2 mM $CaCl_2$ and 0.12 mM $K_2C_2O_4$) at *IS* = 0.15 M and pH = 7.0. Inset shows a magnified area marked by a yellow dashed rectangle to indicate the presence of a typical COM crystal. White dashed lines and arrows demonstrate the growth of COM with elongated crystalline faces.

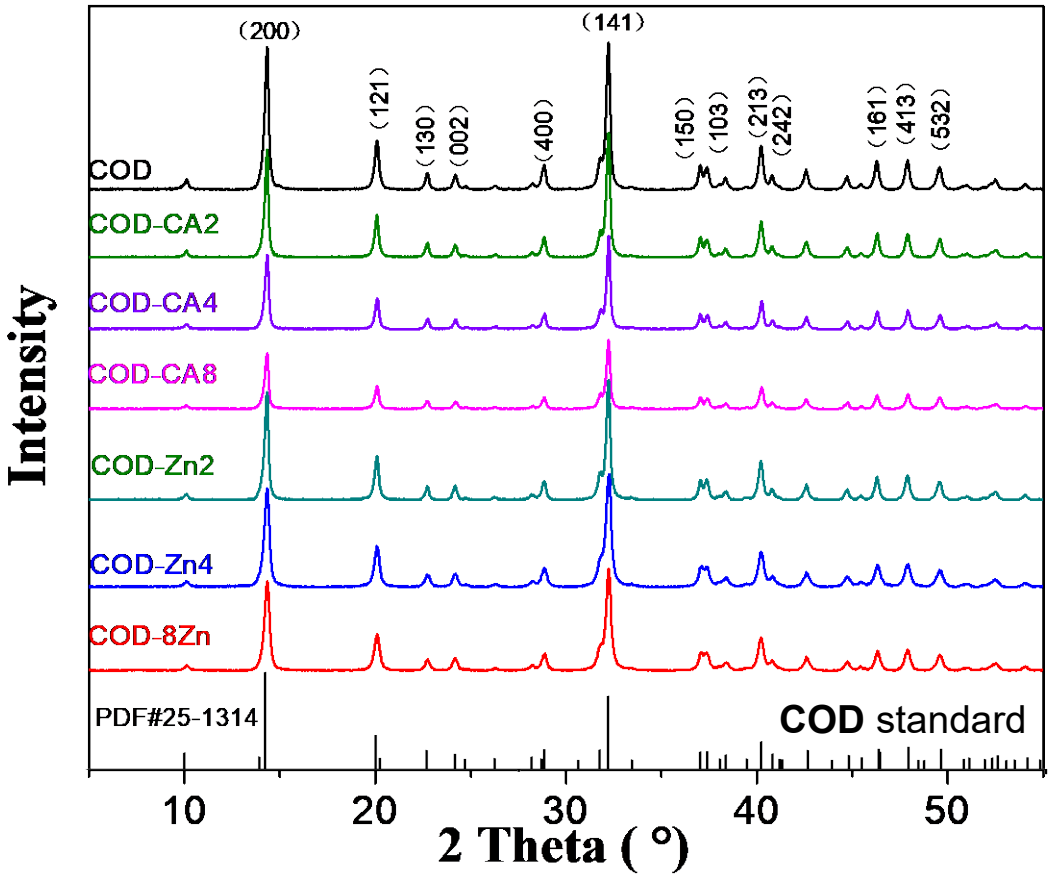

Figure S8. XRD patterns of COD with different amounts of citrate or Zn^{2+}.

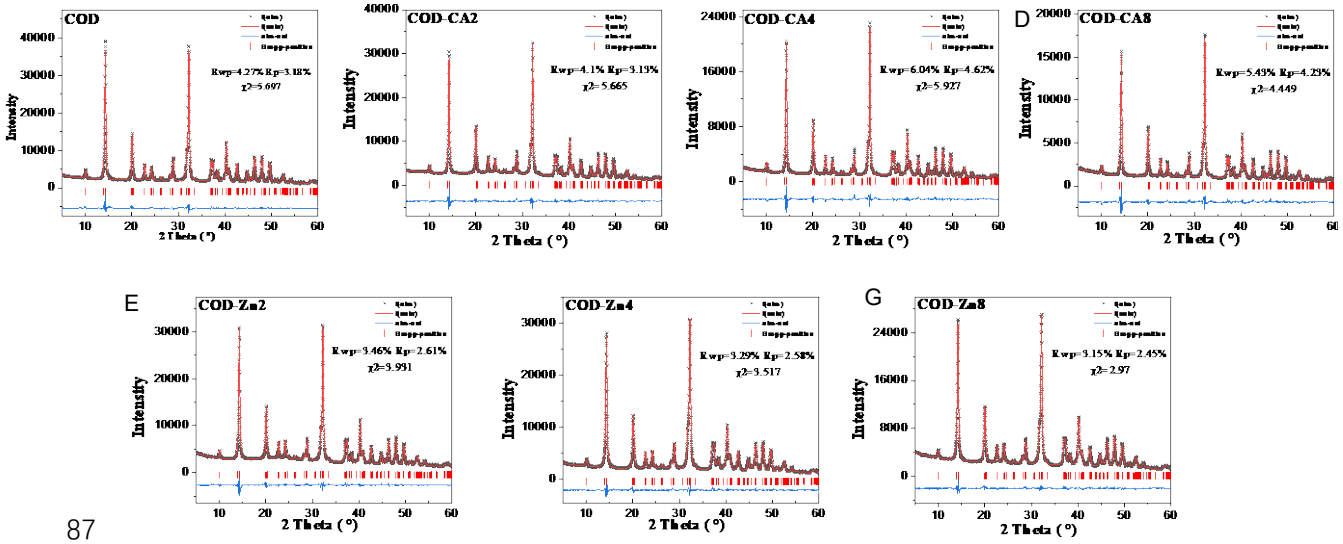

87

88 **Figure S9.** The observed and calculated XRD patterns after Rietveld refinement for the

89 crystallization products of (A) COD, (B) COD-CA2, (C) COD-CA4, (D) COD-CA8,

90 (E) COD-Zn2, (F) COD-Zn4, and (G) COD-Zn8. The observed and calculated

91 intensities are represented by the black fork types and the red solid line, respectively.

92 The blue line at the bottom shows the fitting residual difference. The Bragg positions

93 are represented by red ticks.

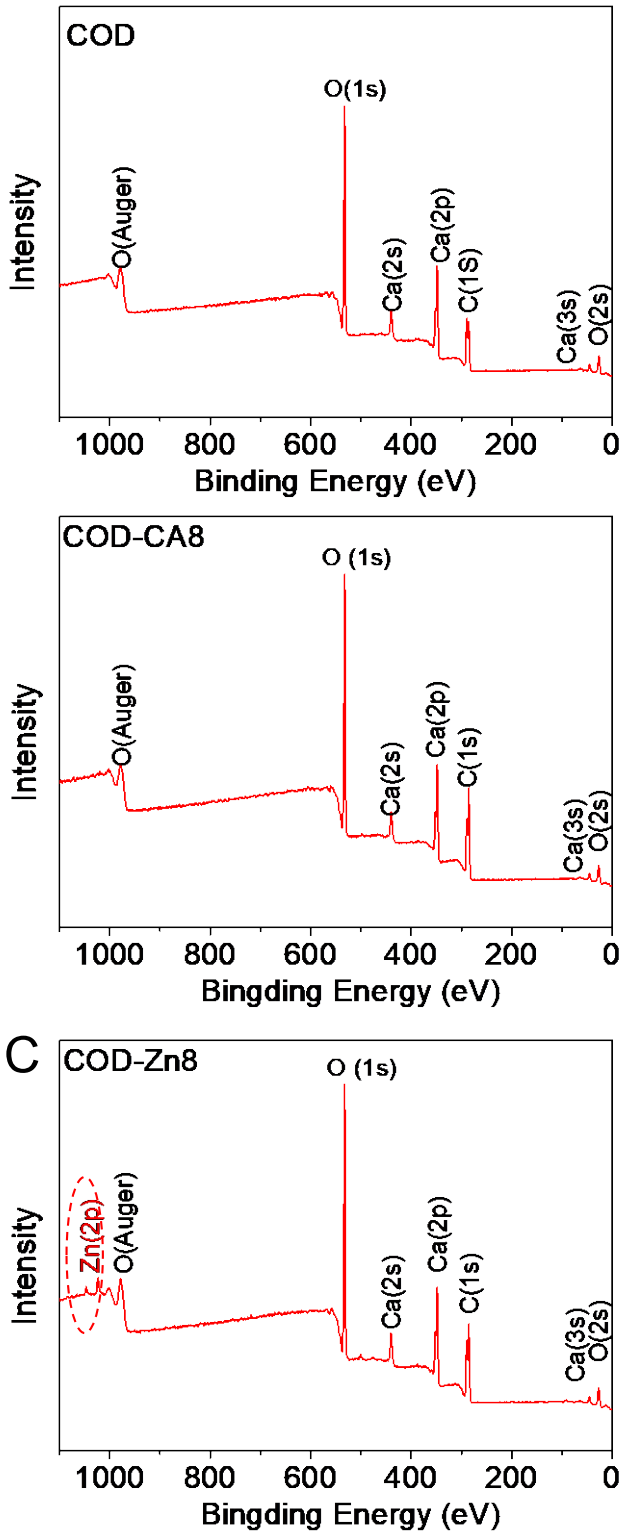

Figure S10. XPS general spectra of (A) COD, (B) COD-CA8, and COD-Zn8, showing that Ca, C and O are present in all samples. Red dashed circle in (C) emphasizes the presence of Zn in COD-Zn8.